Inorganic Chemistry

Article

Polyoxometalate-Based Frameworks as Adsorbents for Drug of Abuse Extraction from Hair Samples

Shadi Derakhshanrad, Masoud Mirzaei,* Carsten Streb,* Amirhassan Amiri, and Chris Ritchie*

Cite This: https://dx.doi.org/10.1021/acs.inorgchem.0c02769
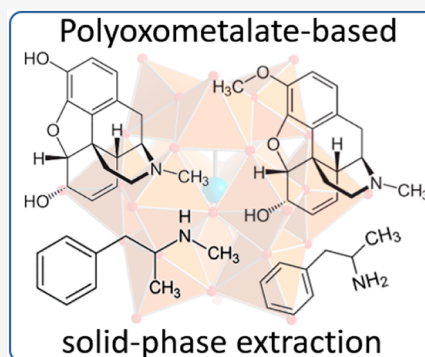
Read Online

ACCESS | Metrics & More | Article Recommendations | Supporting Information

ABSTRACT: The linkage of molecular components into functional heterogeneous framework materials has revolutionized modern materials chemistry. Here, we use this principle to design polyoxometalate-based frameworks as high affinity adsorbents for drugs of abuse, leading to their application in solid-phase extraction analysis. The frameworks are assembled by the reaction of a Keggin-type polyanion, $[SiW_{12}O_{40}]^{4-}$, with lanthanoids Dy(III), La(III), Nd(III), and Sm(III) and the multidentate linking ligand 1,10-phenanthroline-2,9-dicarboxylic acid (H$_2$PDA). Their reaction leads to the formation of crystalline 1D coordination polymers. Because of the charge mismatch between the lanthanoids (+3) and the dodecasilicotungstate (−4), we observe incorporation of the PDA^{2-} ligands into crystalline materials, leading to four polyoxometalate-based frameworks where Keggin-type heteropolyanions are linked by cationic $\{Ln_n(PDA)_n\}$ groups (Ln = Dy (**1**), La (**2**), Nd (**3**), and Sm (**4**)). Structural analysis of the polyoxometalate-based frameworks suggested that they might be suitable for surface binding of common drugs of abuse via supramolecular interactions. To this end, they were used for the extraction and quantitative determination of four model drugs of abuse (amphetamine, methamphetamine, codeine, and morphine) by using micro-solid-phase extraction (D-μSPE) and high-performance liquid chromatography (HPLC). The method showed wide linear ranges, low limits of detection (0.1−0.3 ng mL^{-1}), high precision, and satisfactory spiked recoveries. Our results demonstrate that polyoxometalate-based frameworks are suitable sorbents in D-μSPE for molecules containing amine functionalities. The modular design of these networks could in the future be used to expand and tune their substrate binding behavior.

1. INTRODUCTION

The past decade has seen tremendous progress in the development and use of crystalline framework materials that contain polyoxometalates either as anionic guests within the framework pores or as structural building block within the framework itself.[1−3] Structural analysis of these polyoxometalate-based frameworks suggested their use in applications such as sequestration and extraction.[4] The synthesis or "self-assembly" of materials of this type can be achieved by using a variety of protocols and componentry, including, the use of preformed POM precursors or the generation of the polyanion *in situ*. Linkage of the POM by using one or more of the following (e.g., transition metals, lanthanoids, main group elements, and organic linkers) enables the merging of the component properties and can offer a facile route to crystalline POM-based materials for technologically relevant applications.[5,6] In recent years, POMs have been incorporated into organic−inorganic frameworks as guests or templates to construct novel hybrid materials that have attracted considerable scientific attention in the fields of environmental remediation, pollutant removal, and extraction methods.[4,7−9] This merging of organic and inorganic componentry has led to new properties such as large pores with high specific surface area, opening new opportunities in separation and adsorption technologies.[4,10−13]

Herein, we report the synthesis and characterization of four 1D framework materials together with their application as solid sorbents for the extraction of four model drugs of abuse (amphetamine, methamphetamine, codeine, and morphine) from hair samples using dispersive micro-solid-phase extraction (D-μSPE). This concept based on the well-documented observation that organic molecules can interact and bind to POMs by electrostatics, hydrogen bonding, or multiple weak (e.g., van der Waals or dispersion) interactions is well documented.[14]

We propose that this concept can be harnessed for the binding of analytes, e.g., pharmaceuticals or drugs, which feature a positive charge (e.g., when protonated) or hydrogen-bonding site, so that the cationic analyte binds by electrostatic, dipolar, and/or hydrogen-bonding interactions to the anionic POM surface sites.[5,6,15,16] Prime examples for suitable substrates are opiates and amphetamines which are widely abused drugs and

Table 1. Molecular Structures and Chemical Properties of the Target Drugs

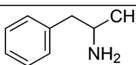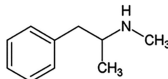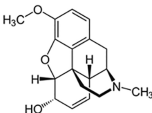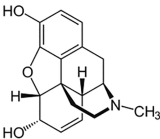| Drugs	Molecular structure	pK_a	$\log K_{ow}$
Amphetamine		9.9	1.76
Methamphetamine		9.87	2.07
Codeine		8.2	1.19
Morphine		8.21	0.89

Table 2. Crystal Data for 1−4

	1	2	3	4
empirical formula	$C_{42}H_{60}N_6NaO_{82}SiDy_3W_{12}$	$C_{56}H_{40}N_8O_{154}Si_2La_6W_{24}$	$C_{28}H_{38}N_4O_{75}SiNd_3W_{12}$	$C_{56}H_{82}N_{12}Na_2O_{158}Si_2Sm_6W_{24}$
M_r (g mol^{-1})	4527.40	8591.00	4297.63	8867.99
temperature (K)	130	130	130	130
crystal system	trigonal	monoclinic	monoclinic	monoclinic
space group	$R3$	Pc	$P2_1/c$	$P2_1/c$
a (Å)	20.3329(3)	13.2137(2)	13.1840(2)	13.0615(2)
b (Å)		25.9371(4)	26.5991(3)	26.1386(4)
c (Å)	18.7830(3)	24.4190(3)	24.3955(3)	24.1245(3)
β (deg)		103.369(1)	102.768(1)	101.6169(14)
crystal size (mm)	$0.07 \times 0.05 \times 0.03$	$0.22 \times 0.08 \times 0.05$	$0.16 \times 0.10 \times 0.08$	$0.14 \times 0.04 \times 0.02$
V (Å^3), Z	6725.0(2), 1	8142.2(2), 2	8343.53(19), 4	8067.6(2), 2
μ (mm^{-1})	42.00	44.63	44.825	48.07
T_{min}, T_{max}	0.414, 0.646	0.021, 0.324	0.038, 0.223	0.116, 0.756
measured, independent and observed reflns	16473, 5164, 5109	43389, 20705, 18345	34264, 17229, 15297	43644, 13219, 11185
R_{int}	0.026	0.052	0.067	0.077
$(\sin \theta/\lambda)_{max}$ (Å^{-1})	0.632	0.633	0.632	0.587
$R[F^2 > 2\sigma(F^2)]$, $wR(F^2)$, S	0.025, 0.066, 1.06	0.074, 0.217, 1.03	0.069, 0.198, 1.06	0.083, 0.214, 1.10
reflns, parameters, restraints	5164, 426, 1	20705, 1691, 2	17229, 1121	13219, 1116, 357
$\Delta\rho_{max}$, $\Delta\rho_{min}$ (e Å^{-3})	1.09, −2.31	6.91, −3.70	7.82, −3.73	4.98, −2.83
absolute structure parameter	0.016(4)	0.053(10)		
CCDC no.	1842657	1897934	1897935	1897937

contain amines with high pK_a values and are therefore easily protonated (Table 1). Quantitative analysis of these kinds of drugs relies on hair analysis as a convenient method of drug monitoring. Compared with the determination of drugs in the blood and urine, hair analysis has advantages such as simple sample preservation, noninvasive sample collection, and long-term stability of the analyte in hair.[17,18] Disadvantages include external contamination (particularly important for smoked drugs), low concentration of analytes, complex matrices, and the limited sample size, resulting in the need for substantial sample treatment prior to analysis.[19−21] To this end, dispersive micro-solid-phase extraction (D-μSPE) has emerged as a powerful miniaturization concept based on solid-phase extraction (SPE) techniques. D-μSPE exhibits significant advantages over tradi-tional SPE with respect to short extraction time, simple procedure, and low sample and solvent consumption.[22−28] Given the importance of the analyte−adsorbent interactions, the

design of advanced adsorbents for the detection of pharma-ceuticals and in particular frequently abused substances is a current research focus.

Here, we propose the use of POMs embedded in hybrid organic−inorganic frameworks as suitable binding sites to extract and preconcentrate highly basic drugs of abuse, enabling their facile subsequent analysis by D-μSPE and high-perform-ance liquid chromatography (HPLC). POMs are polyanionic molecular metal oxide clusters, formed by the acid-driven condensation of small metal oxo precursors in aqueous solution.[29,30] The prime POM prototype is the plenary Keggin anion, $[X^{n+}M_{12}O_{40}]^{(8−n)−}$ (X: e.g., B, Si, P; M: e.g., Mo, W), whose versatile chemistry has been explored in a variety of fields.[31] POMs are currently used in a wide range of applications and are therefore of general scientific interest across numerous fields of research including biochemistry, magnetism, nano-structured materials, energy conversion/storage, and cataly-

sis.[32−41] This work is based on the recent report by some of us that Keggin anions can be linked into framework materials by using lanthanide cations and organic phenanthroline dicarboxylate ligands.[44]

2. EXPERIMENTAL SECTION

Materials and Instruments. All chemicals were purchased commercially (reagent grade) and were used without further purification, except for 1,10-phenanthroline-2,9-dicarbaldehyde dioxime (H$_2$phendox or PDOX) which was synthesized according to a reported procedure.[42,43] The drugs including amphetamine, methamphetamine, codeine, and morphine were obtained from Sigma-Aldrich (St. Louis, MO) (see Table 1). Standardized stock solutions were prepared at 10 ng mL^{-1} levels in HPLC-grade methanol and stored at 4 °C. The analysis solutions were obtained by appropriate dilution of the stock standard solutions with deionized water. Hair samples were cut as close as possible to the scalp in the posterior apex with a scissors. Drug-free hair was obtained from healthy volunteers with no known exposure to drugs of abuse. The drug-containing hair samples were received from Ebnesina Hospital (Mashhad, Iran). Elemental analyses (CHN) were performed by using a Thermo Finnigan Flash-1112EA microanalyzer. The IR spectra were recorded in the range 4000−400 cm^{-1} on a Buck 500 IR spectrometer with the sample prepared as a pressed KBr pellet. A summary of the crystallographic data and the structure refinements are provided in Table 2. Chromatographic separations were performed with a Knauer HPLC instrument equipped with a UV detector. The target analytes were separated by using an ODS3 column (4.6 mm ID × 250 mm length, 5 μm particle diameter). The mobile phase (flow rate of 1.0 mL min^{-1}) was a mixture of 0.05 M aqueous phosphate buffer (pH 4) and acetonitrile (30:70 v/v) with isocratic elution. The wavelength of the UV detector was set to 210 nm.

Synthesis and Characterization. *Synthesis of Hybrid 1.* The synthetic procedure and structure of **1** were reported previously by some of us.[44] Anal. Calcd for C$_{42}$H$_{60}$N$_6$NaO$_{82}$SiDy$_3$W$_{12}$: C, 11.13; H, 1.32; N, 1.85; Na, 0.50; Si, 0.61; Dy, 10.76; W, 48.50%. Found: C, 11.10; H, 1.24; N, 1.78; Na, 0.47; Si, 0.58; Dy, 10.45; W, 48.44%. IR (KBr pellet, cm^{-1}): 3423, 1613, 1568, 1468, 1388, 1307, 967, 914, 789, 712 (Figure S11b).

Synthesis of Hybrid 2. This hybrid framework was prepared similarly to **1**, except that La(NO$_3$)$_3$·6H$_2$O (54 mg, 0.125 mmol) was used instead of Dy(NO$_3$)$_3$·6H$_2$O. Yellow plate crystals were obtained in 57% yield (based on W). Anal. Calcd for C$_{56}$H$_{40}$N$_8$O$_{154}$Si$_2$La$_6$W$_{24}$: C, 7.82; H, 0.46; N, 1.30; Si, 0.65; La, 9.70; W, 51.40%. Found: C, 7.95; H, 0.53; N, 1.32; Si, 0.62; La, 9.87; W, 51.77%. IR (KBr pellet, cm^{-1}): 3432, 1733, 1630, 1606, 1452, 1378, 1209, 916, 789, 711 (Figure S11c).

Synthesis of Hybrid 3. This hybrid framework was prepared similarly to **1**, except that Nd(NO$_3$)$_3$·6H$_2$O (55 mg, 0.125 mmol) was used instead of Dy(NO$_3$)$_3$·6H$_2$O. Yellow needle crystals were obtained in 48% yield (based on W). Anal. Calcd for C$_{28}$H$_{38}$N$_4$O$_{75}$SiNd$_3$W$_{12}$: C, 7.82; H, 0.88; N, 1.30; Si, 0.65; Nd, 10.05; W, 51.10%. Found: C, 7.96; H, 0.95; N, 1.43; Si, 0.67; Nd, 9.96; W, 51.28%. IR (KBr pellet, cm^{-1}): 3374, 1596, 1562, 1463, 1388, 1392, 1306, 963, 914, 796, 715 (Figure S11d).

Synthesis of Hybrid 4. This hybrid framework was prepared similarly to **1**, except that Sm(NO$_3$)$_3$·6H$_2$O (56 mg, 0.125 mmol) was used instead of Dy(NO$_3$)$_3$·6H$_2$O. Yellow needle crystals were obtained in 52% yield (based on W). Anal. Calcd for C$_{56}$H$_{82}$N$_{12}$Na$_2$O$_{158}$Si$_2$Sm$_6$W$_{24}$: C, 7.58; H, 0.92; N, 1.90; Na, 0.52; Si, 0.63; Sm, 10.15; W, 49.53%. Found: C, 7.65; H, 0.95; N, 1.94; Na, 0.58; Si, 0.66; Sm, 10.25; W, 50.20%. IR (KBr pellet, cm^{-1}): 3412, 1613, 1564, 1466, 1389, 1308, 965, 914, 794, 712 (Figure S11e).

Hair Samples. The hair specimen was washed with methanol, acetone, and deionized water to remove contamination on the hair surface. After drying, the hair was cut into very fine pieces, weighed (∼50 mg), and digested in methanol at 55 °C for 5 h. The extracted compounds were filtered, then dried under a stream of nitrogen gas, and finally redissolved in 5.0 mL of deionized water. Also, for spiking the hair samples, the appropriate amounts of standard solutions of target drugs were added to the pretreated hair samples.

Extraction Procedure. 5.0 mL of the pretreated hair sample containing a certain amount of target drugs was adjusted to pH 5 (phosphate buffer) and then placed in a glass vial. 30 mg of the adsorbent (**1−4**) was added to the sample and sonicated for 5 min. Then, the mixture was centrifuged and the supernatant discarded. Thereafter, the adsorbed analytes were eluted with 200 μL of 20% ammonia in acetonitrile under sonication, for 2 min. After centrifuging the solution, the desorption solvent was transferred to another vial and dried by a gentle flow of nitrogen gas. Then, the residue was redissolved in 20 μL of acetonitrile solvent and analyzed by HPLC.

3. RESULTS AND DISCUSSION

Synthesis. The synthesis of the polyoxometalate-based frameworks was achieved by the hydrothermal reaction of lanthanide salts, organic ligands, and H$_4$[SiW$_{12}$O$_{40}$]·xH$_2$O. See the Experimental Section for details. Control of solution pH (between pH 3.0−3.5) and temperature (130 °C) is key to obtaining the hybrid materials reported herein. The reactions gave crystalline products suitable for structure determination using single-crystal X-ray diffraction (SCXRD) analysis. Powder X-ray diffraction further demonstrated the bulk purity of **1−4**.

Structure Description of 1−4. SCXRD data, data collection, and structure refinement details are summarized in Table 2. Diffraction data of the polyoxometalate-based frameworks were collected on an Agilent SuperNova single-crystal X-ray diffractometer with graphite-monochromated Cu Kα radiation ($\lambda \sim 1.54$ Å) at 130 K (Table 2). The structures for **1−4** were solved by direct methods using the program SHELXS and refined by full-matrix least-squares methods on F^2 using SHELXL. Note that compound **1** had been reported previously by some of us.[44] Multiscan absorption correction was applied. Crystallographic details can be found in the CIF files. The CIF files are available free of charge from the Cambridge Crystallographic Data Centre CCDC.

Structural analysis of the SCXRD data indicates **1−4** all contain the silicotungstate Keggin polyanion [SiW$_{12}$O$_{40}$]$^{4-}$ (hereafter: W$_{12}$). The crystal structure of **1** is described in a previous publication.[44] It is worth mentioning that the range of the Ln−O distances are consistent with effects of the lanthanide contraction (ionic radius: La^{3+} > Nd^{3+} > Sm^{3+} > Dy^{3+}). Moreover, in all four polyoxometalate-based frameworks, we observe distinct Ln−O distances: Ln−O(H$_2$O) > Ln−O$_{terminal}$ > Ln−O$_{PDA}$, highlighting different bonding strengths in the order O$_{PDA}$ > O$_t$ > O(H$_2$O).

The hybrid frameworks are formed by linkages between the PDA^{2-} ligands Ln(III) ions and Keggin polyanions in tetradentate chelating-bridging coordination mode, resulting in 1D zigzag Ln−PDA complex chains, namely, −Ln1(PDA)− Ln2−Ln1(PDA)−. The zigzag Ln−PDA complex chains are joined together by the coordination of [La$_2$(PDA)$_2$] units in **2** and **3** and [Na$_2$La$_2$(PDA)$_2$] units in **4**.

Hybrid 2. A view of the asymmetric unit of **2** is presented in Figure S4. Hybrid **2** crystallized in the monoclinic space group *Pc*. As shown in Figures S5 and S6, the compound can be described as a 1D coordination polymer based on two Keggin polyanions, [SiW$_{12}$O$_{40}$]$^{4-}$, four [La(PDA)]$^+$ fragments, and two La(III) which represent 1D chainlike architecture. The polyanions [SiW$_{12}$O$_{40}$]$^{4-}$ act as monodentate ligands and coordinate to a [La(PDA)]$^+$ fragment via a terminal oxo ligand. The host metal−organic cations are constructed from PDA^{2-} ligands and La(III) centers with slightly different local coordination environments. Each La atom is coordinated with
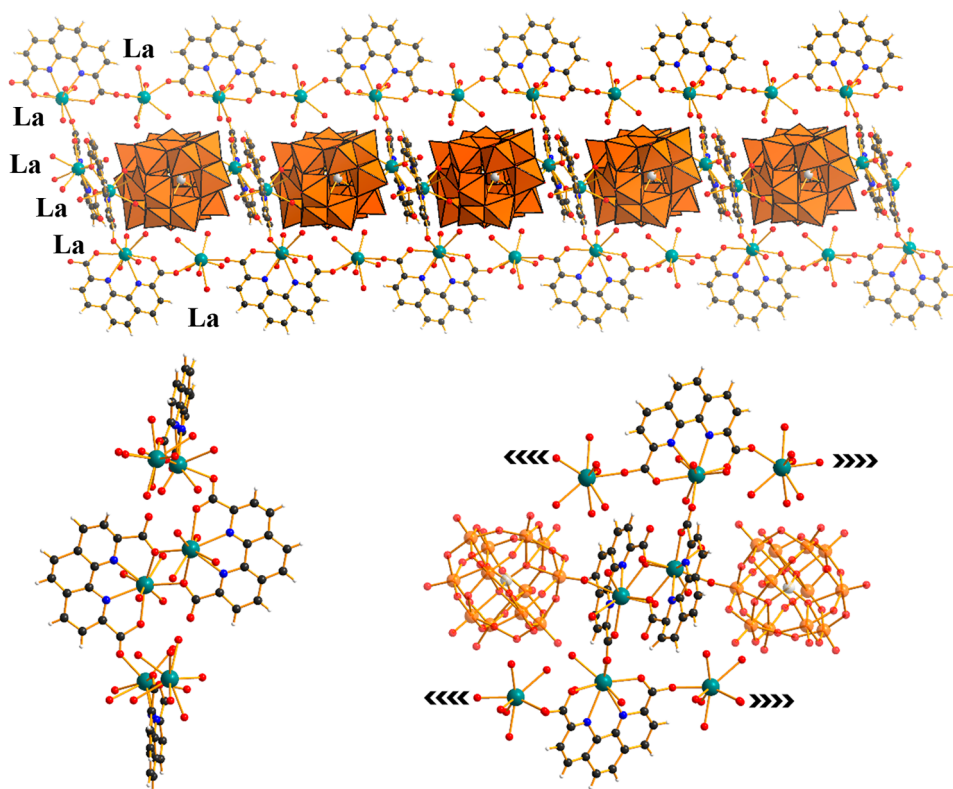
Figure 1. Mixed polyhedral, ball and stick representation of **2** along the crystallographic *c*-axis (top and bottom right) and *a*-axis (bottom left) without polyanions for clarity. C, black; H, white; N, blue; La, teal; O, red; Si, gray; W, orange.
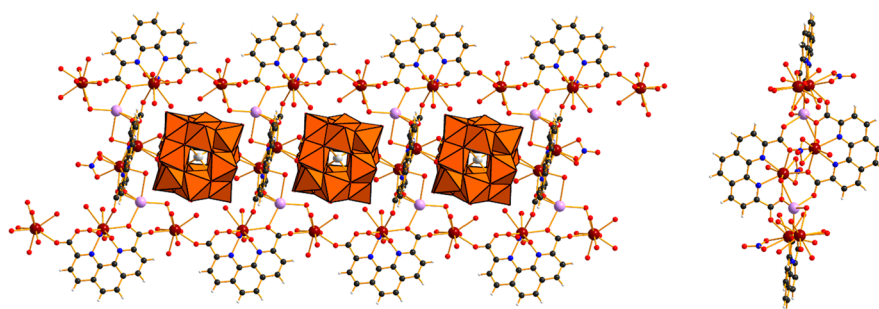
Figure 2. Mixed polyhedral, ball and stick representation of **4**. C, black; H, white; N, blue; Na, pink; O, red; Si, gray; Sm, maroon; W, orange.

different coordination modes that are shown in Figure 1. Two nine-coordinated La(III) atoms (La3 and La4) are linked by two PDA^{2-} ligands through O_1,O_2-bridging mode to generate a $[La_2(PDA)_2]$ unit. In addition, adjacent $[La_2(PDA)_2]$ units are linked by two other La(III) atoms through carboxylate oxygen atoms from PDA^{2-} to form the host cation. La2 is coordinated to two nitrogen and two carboxylate oxygen atoms from PDA^{2-} and five oxygen atoms from coordinated water molecules. Also, La1 is connected to two carboxylate oxygen atoms from PDA^{2-} and six oxygen atoms from coordinated water molecules. Finally, La3 and La4 are linked by the same coordination mode. They are coordinated to two nitrogen and three carboxylate oxygen atoms from two different PDA^{2-} ligands and oxygen atoms from coordinated water molecules.

Hybrid 3. The host−guest assemblies in **2** and **3** are similar. As shown in Figure S7, the asymmetric unit of **3** is composed of one Keggin anion, two crystallographically independent PDA^{2-} ligands, three crystallographically unique Nd^{3+} ions, and numbers of coordinated and uncoordinated water molecules.

A remarkable feature of **3** is that each Keggin cluster connects to one Nd(III) ion (Figure S9). In **3**, crystallographically independent Nd3, Nd1, and Nd2 are 8-, 9-, and 10-coordinated, displaying distorted square antiprism, distorted monocapped square antiprism, and distorted dicapped square antiprism coordination geometry, respectively. It should be noted that in both polyoxometalate-based frameworks the 1D chain is stacked. The metal−organic fragment in **3** is a supramolecular isomer of that in **2**, and the basic Nd(III)-PDA^{2-} unit is $[Nd_2(PDA)_2]$. The $[Nd_2(PDA)_2]$ units are further connected by other PDA^{2-} ligands and La(III) atoms. It is interesting to note that a chain presents a wave-shaped single strand viewed along the crystallographic *b*-axis (Figure S8). In addition, Nd−$(O)_2$−Nd is a direct ligand bridge which links the chains.

Hybrid 4. **4** is structurally closely related to **3** and crystallizes in a monoclinic crystal system with the space group $P2_1/c$. The asymmetric unit **4** is composed of one W_{12} cluster, two crystallographically independent PDA^{2-} ligands, three crystallographically unique Sm^{3+} ions, two Na$^+$ ions, and numbers of

coordinated and uncoordinated water molecules (Figure S9). Crystal structure analysis reveals that compound **4** consists of three main parts: $[SiW_{12}O_{40}]^{4-}$ polyoxoanion, $\{Na_2Sm_2(PDA)_2\}$ groups, and Sm3−Sm2(PDA)−Sm3 linear chains. In compound **4**, crystallographically independent Sm1, Sm2, and Sm3 are all 11-coordinated, displaying a distorted monocapped pentagonal antiprism coordination geometry. As shown in Figure 2, there are three types of Sm ions (Sm1, Sm2, and Sm3) in **4**: Sm1 is linked with other Sm1 atoms through two bridging oxygen and three nitrogen atoms from PDA^{2-}, Na$^+$ ion from NaOH, a terminal oxygen atom from POM, and other oxygen atoms from coordination H$_2$O molecules. The Sm2 atom displays 11-coordination geometry established by three nitrogen atoms (N4, N5, and N6), two carboxylate oxygen atoms (O51 and O53) from PDA^{2-}, and the other oxygen atoms from coordinated water molecules. The last type of Sm(III) (Sm3) ions is connected to two carboxylate oxygen atoms (O54 and O52) from PDA^{2-} to construct PDA−Sm3−PDA linear chains, Na$^+$ ion from NaOH, and the other oxygen atoms from coordinated water molecules (Figure 2 and Figure S10).

Drug Adsorption Experiments for Ln-Functionalized Polyoxotungstates−Organic Frameworks. As outlined in the Introduction, the organic−inorganic nature of **1**−**4** led us to propose them as suitable adsorbents for organic drug molecules. To this end, we explored the extraction performance of the four polyoxometalate-based frameworks toward four model drugs of abuse (i.e., amphetamine, methamphetamine, codeine, and morphine) in hair samples. As all analytes tested feature basic amine groups, their protonation degree can be controlled by the solution pH. We propose that this introduction of a cationic charge allows increased interactions of the model drugs with the adsorbent surface. To this end, we quantitatively explored the extraction performance of **1**−**4** (Figure 3). As can be seen in

Figure 3. Extraction efficiency of **1**−**4** for the D-μSPE of the target drugs.

Figure 3, the order of the extraction efficiency for the D-μSPE of the target drugs is as follows: **4** > **2** > **3** > **1** (Figure 3). Notably, despite their different structures, the extraction recoveries (i.e., binding affinity of the drugs to the framework materials) are all in a similar range. We suggest that this could be related to the fact that all drugs have similar pK_a values (Table 1) and that electrostatic interactions rather than specific structural features control the binding of the substrate to the framework.

Based on this initial finding, the Sm-containing **4** was used for more detailed extraction analyses. To investigate the best condition for the extraction of target drugs, several parameters such as the amount of adsorbent (10−50 mg), desorption conditions (eluent, eluent volume, and elution time), extraction time (1−7 min), pH (3−6), and salt effect (0−10% w/v) were studied. The general trends are that higher amount of adsorbent and longer elution/extraction times result in higher recoveries. With respect to pH value, we suggest that two trends could lead to the data observed in Figure 4e: at high pH values, the analytes are less protonated, thereby lowering the binding affinity to the frameworks. At low pH, surface protonation of the frameworks could become possible, thereby lowering electrostatic inter-actions with the analyte. A similar argument can be made for the effects of NaCl addition: we suggest that the presence of NaCl introduces competing Na$^+$ cations which can also bind to the framework surface. In addition, solution interactions between the analytes and the NaCl ions are possible. In addition, modification of the ionic strength of the solvent can lead to an increased solubility of the analytes and therefore reduce their binding to the framework materials. The following experimental conditions yielded the best results: (a) 30 mg of the adsorbents (Figure 4a); (b) eluent, acetonitrile/ammonia (80/20 v/v) (Figure 4b); (c) volume of the eluent, 200 μL; (d) elution time, 2 min (Figure 4c); (e) extraction time, 5 min (Figure 4d); (f) sample pH, 5 (Figure 4e); and without addition of NaCl (Figure 4f).

Method Validation. Under optimized conditions, we then examined the linearity, the lower limit of detection (LOD), precision, and extraction recovery (%) of the D-μSPE-HPLC-UV method (Table 3). The calibration curve for HPLC-UV analysis was acquired by using different drug concentrations solution. The good linearity was achieved for all of the analytes, with correlation coefficients (r) higher than 0.9959, in the range 0.3−300 ng mL^{-1} (0.7−300 ng mL^{-1} for amphetamine, 0.3−300 ng mL^{-1} methamphetamine, and 1.0−200 ng mL^{-1} for codeine and morphine). The LOD was defined as the lowest concentration at which a signal-to-noise ratio of 3 (S/N = 3) was observed which ranged from 0.1 to 0.3 ng mL^{-1}. The repeatability of the method was investigated in hair samples at two concentration levels (5.0 and 50 ng mL^{-1}). As shown in Table 3, the relative standard deviation (RSD) was in the range 4.1−5.5%, which is satisfactory. The extraction recoveries obtained were in the range 78.6−84.1%.

Analysis of Real Samples. To assess the applicability of the proposed method, the D-μSPE-HPLC-UV method was applied to extract and determine of amphetamine, methamphetamine, codeine, and morphine in the hair of drug abusers. Real hair samples of drug abusers were obtained from a Hospital in Mashhad, Iran. Five hair samples were collected and analyzed by the D-μSPE-HPLC-UV method. These samples were further confirmed by LC-MS. The results from each sample are listed in Table S1. To investigate the effect of the matrix, the relative recovery of the method was studied by spiking of the target analytes at two concentration levels (5.0 and 50 ng mL^{-1}) to each real sample. As shown in Table S1, the relative recoveries were in the range 93.4−98.2% with an RSD of 5.9−7.3%. Note that at this stage we do not observe a clear correlation between adsorptive properties and crystal structure polymorph of polyoxometalate-based frameworks **1**−**4**, and further (kinetic) binding studies are required to gain more insights into the role of the exact structure on the substrate binding properties.

4. CONCLUSION

In this work, we report the first example of the use of polyoxometalate-based modular organic−inorganic frameworks

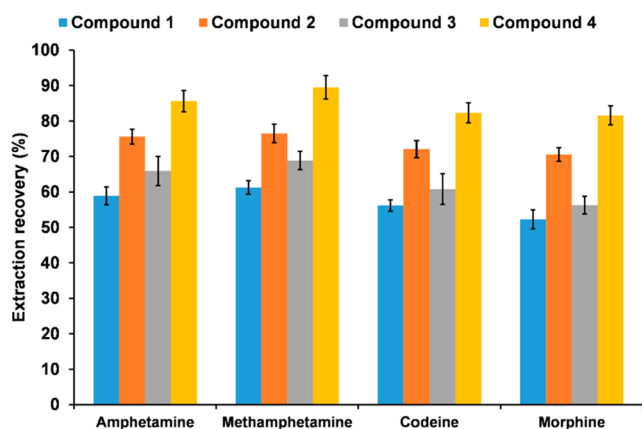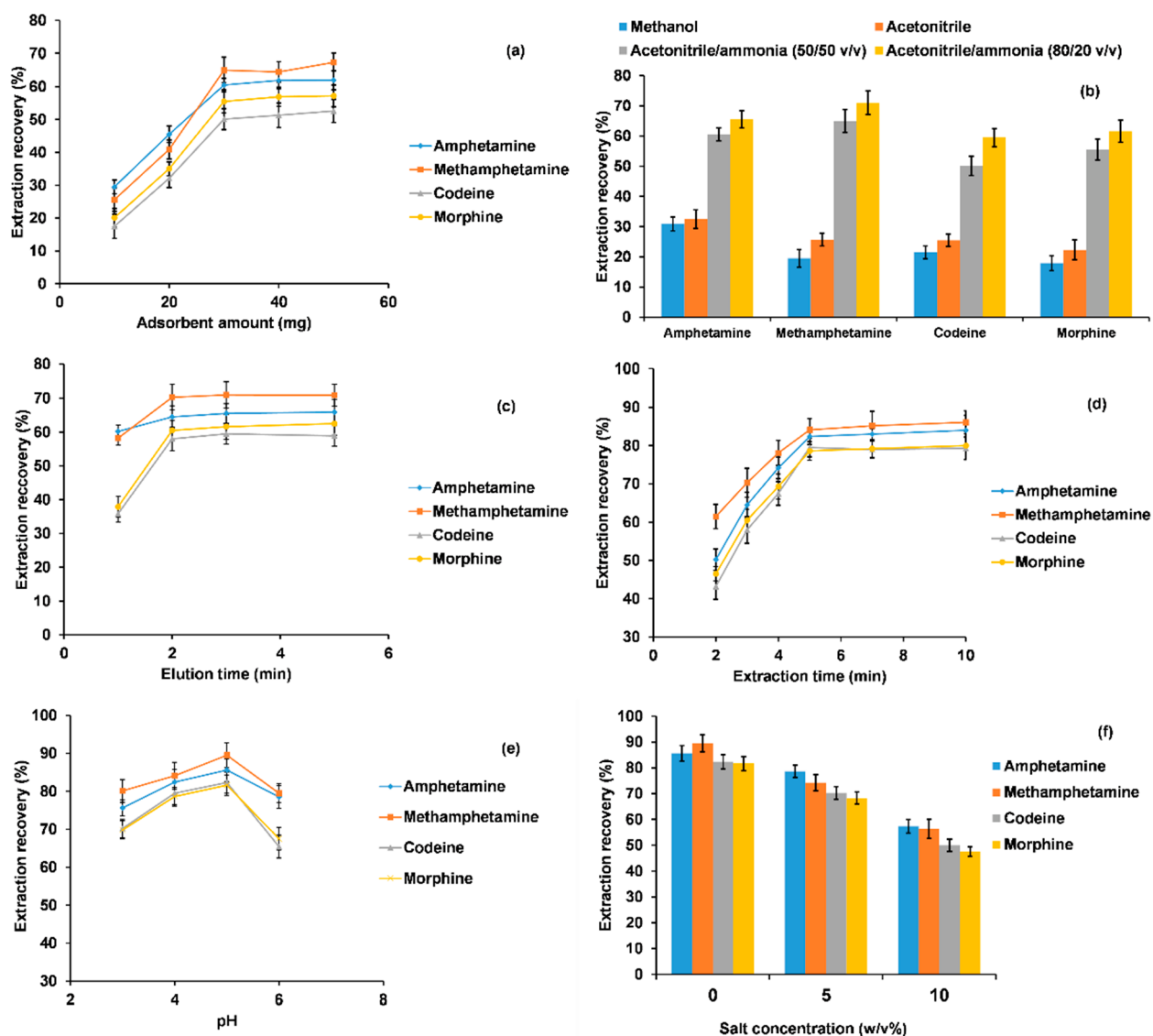**Figure 4.** Effects of (a) adsorbent amount, (b) eluent, (c) elution time, (d) extraction time, (e) pH of sample, and (f) effect of NaCl concentration on the extraction performance.

Table 3. Analytical Figures of Merit of the D-μSPE Method of the Drugs of Abuse

analyte	linear range (ng mL^{-1})	LOD (ng mL^{-1})	correlation coeff (r)	ER (%)	precision 5.0 ng mL^{-1}	precision 50 ng mL^{-1}
amphetamine	0.7–300	0.2	0.9975	85.6	5.1	4.7
methamphetamine	0.3–300	0.1	0.9966	89.5	4.9	4.4
codeine	1.0–200	0.3	0.9988	82.3	4.5	4.1
morphine	1.0–200	0.3	0.9959	81.6	5.5	4.9

for the extraction and quantitative analysis of drugs of abuse. Four 1D coordination polymers based on Keggin-type heteropolytungstates linked by lanthanoids (Dy, Sm, La, and Nd) and organic PDA^{2-} ligands were synthesized and used as adsorbents for the D-μSPE extraction and adsorption of four drugs of abuse (amphetamine, methamphetamine, codeine, and morphine). We report high extraction efficiency, wide linear range, and low limits of detection, making this an intriguing new application field for polyoxometalate-based heterogeneous materials, even when by using complex sample matrices. Future work will explore in more detail the interaction between the POM and the drug molecules and will assess and optimize the materials for usage under "real-life" conditions.

■ ASSOCIATED CONTENT

Ⓢ Supporting Information

The Supporting Information is available free of charge at https://pubs.acs.org/doi/10.1021/acs.inorgchem.0c02769.

    Figures S1−S11, IR spectra, and SCXRD analyses of **1−4** (PDF)

■ AUTHOR INFORMATION

Corresponding Authors

Masoud Mirzaei − *Department of Chemistry, Faculty of Science, Ferdowsi University of Mashhad, Mashhad 9177948974, Iran;* orcid.org/0000-0002-7256-4601; Email: mirzaeesh@um.ac.ir

Carsten Streb − *Institute of Inorganic Chemistry I, Ulm University, 89081 Ulm, Germany;* orcid.org/0000-0002-5846-1905; Email: carsten.streb@uni-ulm.de

Chris Ritchie − *School of Chemistry, Monash University, Clayton 3800, Victoria, Australia;* orcid.org/0000-0002-1640-6406; Email: Chris.Ritchie@monash.edu

Authors

Shadi Derakhshanrad − *Department of Chemistry, Faculty of Science, Ferdowsi University of Mashhad, Mashhad 9177948974, Iran*

Amirhassan Amiri − *Department of Chemistry, Faculty of Sciences, Hakim Sabzevari University, Sabzevar 96179-76487, Iran*

Complete contact information is available at:
https://pubs.acs.org/10.1021/acs.inorgchem.0c02769

Notes

The authors declare no competing financial interest.

■ REFERENCES

(1) Miras, H. N.; Vilà-Nadal, L.; Cronin, L. Polyoxometalate based open-frameworks (POM-OFs). *Chem. Soc. Rev.* **2014**, *43* (16), 5679−5699.

(2) Vilà-Nadal, L.; Cronin, L. Design and synthesis of polyoxometalate-framework materials from cluster precursors. *Nat. Rev. Mater.* **2017**, *2* (10), 17054.

(3) Samaniyan, M.; Mirzaei, M.; Khajavian, R.; Eshtiagh-Hosseini, H.; Streb, C. Heterogeneous catalysis by polyoxometalates in metal−organic frameworks. *ACS Catal.* **2019**, *9* (11), 10174−10191.

(4) Bagheri, H.; Zandian, F. K.; Javanmardi, H.; Abbasi, A.; Aqda, T. G. Nanostructured molybdenum oxide in a 3D metal organic framework and in a 2D polyoxometalate network for extraction of chlorinated benzenes prior to their quantification by GC−MS. *Microchim. Acta* **2018**, *185* (12), 536.

(5) Dolbecq, A.; Dumas, E.; Mayer, C. R.; Mialane, P. Hybrid organic−inorganic polyoxometalate compounds: from structural diversity to applications. *Chem. Rev.* **2010**, *110* (10), 6009−6048.

(6) Chen, Q.; Zhang, D.-D.; Wang, M.-M.; Chen, X.-W.; Wang, J.-H. A novel organic−inorganic hybrid polyoxometalate for the selective adsorption/isolation of β-lactoglobulin. *J. Mater. Chem. B* **2015**, *3* (34), 6964−6970.

(7) Ammar, S. H.; Abdulnabi, W. A. Synthesis, characterization and environmental remediation applications of polyoxometalates-based magnetic zinc oxide nanocomposites (Fe₃O₄@ ZnO/PMOs). *Environ. Nanotechnol. Monit. Manag.* **2020**, *13*, 100289.

(8) Sivakumar, R.; Thomas, J.; Yoon, M. Polyoxometalate-based molecular/nano composites: Advances in environmental remediation by photocatalysis and biomimetic approaches to solar energy conversion. *J. Photochem. Photobiol., C* **2012**, *13* (4), 277−298.

(9) Misra, A.; Zambrzycki, C.; Kloker, G.; Kotyrba, A.; Anjass, M. H.; Franco Castillo, I.; Mitchell, S. G.; Güttel, R.; Streb, C. Water Purification and Microplastics Removal Using Magnetic Polyoxometalate-Supported Ionic Liquid Phases (magPOM-SILPs). *Angew. Chem., Int. Ed.* **2020**, *59* (4), 1601−1605.

(10) Liang, S.; Nie, Y.-M.; Li, S.-H.; Zhou, J.-L.; Yan, J. A Comprehensive Study on the Dye Adsorption Behavior of Polyoxometalate-Complex Nano-Hybrids Containing Classic β-Octamolybdate and Biimidazole Units. *Molecules* **2019**, *24* (4), 806.

(11) Chen, Q.; Zhang, D.-D.; Wang, M.-M.; Chen, X.-W.; Wang, J.-H. A novel organic−inorganic hybrid polyoxometalate for the selective adsorption/isolation of β-lactoglobulin. *J. Mater. Chem. B* **2015**, *3* (34), 6964−6970.

(12) Gong, Y.-R.; Chen, W.-C.; Zhao, L.; Shao, K.-Z.; Wang, X.-L.; Su, Z.-M. Functionalized polyoxometalate-based metal−organic cuboctahedra for selective adsorption toward cationic dyes in aqueous solution. *Dalton Trans.* **2018**, *47* (37), 12979−12983.

(13) Farhadi, S.; Amini, M. M.; Dusek, M.; Kucerakova, M.; Mahmoudi, F. A new nanohybrid material constructed from Keggin-type polyoxometalate and Cd (II) semicarbazone Schiff base complex with excellent adsorption properties for the removal of cationic dye pollutants. *J. Mol. Struct.* **2017**, *1130*, 592−602.

(14) Wang, H.; Yan, Y.; Li, B.; Bi, L.; Wu, L. Hierarchical Self-Assembly of Surfactant-Encapsulated and Organically Grafted Polyoxometalate Complexes. *Chem. - Eur. J.* **2011**, *17* (15), 4273−4282.

(15) Yi, F.-Y.; Zhu, W.; Dang, S.; Li, J.-P.; Wu, D.; Li, Y.-h.; Sun, Z.-M. Polyoxometalates-based heterometallic organic−inorganic hybrid materials for rapid adsorption and selective separation of methylene blue from aqueous solutions. *Chem. Commun.* **2015**, *51* (16), 3336−3339.

(16) Jiao, Y.-Q.; Qin, C.; Zang, H.-Y.; Chen, W.-C.; Wang, C.-G.; Zheng, T.-T.; Shao, K.-Z.; Su, Z.-M. Assembly of organic−inorganic hybrid materials constructed from polyoxometalate and metal−1, 2, 4-triazole units: synthesis, structures, magnetic, electrochemical and photocatalytic properties. *CrystEngComm* **2015**, *17* (10), 2176−2189.

(17) Vogliardi, S.; Tucci, M.; Stocchero, G.; Ferrara, S. D.; Favretto, D. Sample preparation methods for determination of drugs of abuse in hair samples: a review. *Anal. Chim. Acta* **2015**, *857*, 1−27.

(18) Kamata, T.; Shima, N.; Sasaki, K.; Matsuta, S.; Takei, S.; Katagi, M.; Miki, A.; Zaitsu, K.; Nakanishi, T.; Sato, T.; Suzuki, K.; Tsuchihashi, H. Time-course mass spectrometry imaging for depicting drug incorporation into hair. *Anal. Chem.* **2015**, *87* (11), 5476−5481.

(19) Duvivier, W. F.; van Putten, M. R.; van Beek, T. A.; Nielen, M. W. (Un) targeted Scanning of Locks of Hair for Drugs of Abuse by Direct Analysis in Real Time−High-Resolution Mass Spectrometry. *Anal. Chem.* **2016**, *88* (4), 2489−2496.

(20) Porta, T.; Grivet, C.; Kraemer, T.; Varesio, E.; Hopfgartner, G. Single hair cocaine consumption monitoring by mass spectrometric imaging. *Anal. Chem.* **2011**, *83* (11), 4266−4272.

(21) Lin, Y.-H.; Lee, M.-R.; Lee, R.-J.; Ko, W.-K.; Wu, S.-M. Hair analysis for methamphetamine, ketamine, morphine and codeine by cation-selective exhaustive injection and sweeping micellar electrokinetic chromatography. *J. Chromatogr. A* **2007**, *1145* (1−2), 234−240.

(22) Maya, F.; Palomino Cabello, C.; Estela, J. M.; Cerdà, V.; Turnes Palomino, G. Automatic in-syringe dispersive microsolid phase extraction using magnetic metal−organic frameworks. *Anal. Chem.* **2015**, *87* (15), 7545−7549.

(23) Tang, S.; Lee, H. K. Application of dissolvable layered double hydroxides as sorbent in dispersive solid-phase extraction and extraction by co-precipitation for the determination of aromatic acid anions. *Anal. Chem.* **2013**, *85* (15), 7426−7433.

(24) Amiri, A.; Baghayeri, M.; Nori, S. Magnetic solid-phase extraction using poly (para-phenylenediamine) modified with magnetic nanoparticles as adsorbent for analysis of monocyclic aromatic amines in water and urine samples. *J. Chromatogr. A* **2015**, *1415*, 20−26.

(25) Alinezhad, H.; Amiri, A.; Tarahomi, M.; Maleki, B. Magnetic solid-phase extraction of non-steroidal anti-inflammatory drugs from environmental water samples using polyamidoamine dendrimer functionalized with magnetite nanoparticles as a sorbent. *Talanta* **2018**, *183*, 149−157.

(26) Amiri, A.; Ghaemi, F.; Maleki, B. Hybrid nanocomposites prepared from a metal-organic framework of type MOF-199 (Cu) and graphene or fullerene as sorbents for dispersive solid phase extraction of polycyclic aromatic hydrocarbons. *Microchim. Acta* **2019**, *186* (3), 131.

(27) Amiri, A.; Tayebee, R.; Abdar, A.; Sani, F. N. Synthesis of a zinc-based metal-organic framework with histamine as an organic linker for the dispersive solid-phase extraction of organophosphorus pesticides in water and fruit juice samples. *J. Chromatogr. A* **2019**, *1597*, 39−45.

(28) Rezvani-Eivari, M.; Amiri, A.; Baghayeri, M.; Ghaemi, F. Magnetized graphene layers synthesized on the carbon nanofibers as novel adsorbent for the extraction of polycyclic aromatic hydrocarbons from environmental water samples. *J. Chromatogr. A* **2016**, *1465*, 1−8.

(29) Hill, C. L. POM-Reviews. *Chem. Rev.* **1998**, *98*, 1−390.

(30) Cronin, L.; Müller, A. Special POM-themed issue. *Chem. Soc. Rev.* **2012**, *41* (22), 7333.

(31) Kondinski, A.; Parac-Vogt, T. N. Keggin Structure, Quō Vādis? *Front. Chem.* **2018**, *6*, 346.

(32) Lotfian, N.; Mirzaei, M.; Eshtiagh Hosseini, H.; Löffler, M.; Korabik, M.; Salimi, A. Two New Supramolecular Hybrids Inorganic-Organic of 12-Silicotungstic Acid Heteropolyoxometalate and Trinuclear Lanthanide Clusters: Syntheses, Structures, and Magnetic Properties. *Eur. J. Inorg. Chem.* **2014**, *2014*, 5908−5915.

(33) Alipour, M.; Akintola, O.; Buchholz, A.; Mirzaei, M.; Eshtiagh-Hosseini, H.; Görls, H.; Plass, W. Size-Dependent Self-Assembly of Lanthanide-Based Coordination Frameworks with Phenanthroline-2,9-dicarboxylic Acid as a Preorganized Ligand in Hybrid Materials. *Eur. J. Inorg. Chem.* **2016**, *2016* (34), 5356−5365.

(34) Arefian, M.; Mirzaei, M.; Eshtiagh-Hosseini, H. Structural insights into two inorganic-organic hybrids based on chiral amino acids and polyoxomolybdates. *J. Mol. Struct.* **2018**, *1156*, 550−558.

(35) Arefian, M.; Mirzaei, M.; Eshtiagh-Hosseini, H.; Frontera, A. A survey of the different roles of polyoxometalates in their interaction with amino acids, peptides and proteins. *Dalton Trans.* **2017**, *46* (21), 6812−6829.

(36) Mirzaei, M.; Eshtiagh-Hosseini, H.; Alipour, M.; Frontera, A. Recent developments in the crystal engineering of diverse coordination modes (0−12) for Keggin-type polyoxometalates in hybrid inorganic−organic architectures. *Coord. Chem. Rev.* **2014**, *275*, 1−18.

(37) Taleghani, S.; Mirzaei, M.; Eshtiagh-Hosseini, H.; Frontera, A. Tuning the topology of hybrid inorganic−organic materials based on the study of flexible ligands and negative charge of polyoxometalates: a crystal engineering perspective. *Coord. Chem. Rev.* **2016**, *309*, 84−106.

(38) Fashapoyeh, M. A.; Mirzaei, M.; Eshtiagh-Hosseini, H.; Rajagopal, A.; Lechner, M.; Liu, R.; Streb, C. Photochemical and electrochemical hydrogen evolution reactivity of lanthanide-function-alized polyoxotungstates. *Chem. Commun.* **2018**, *54*, 10427−10430.

(39) Du, X.; Zhao, J.; Mi, J.; Ding, Y.; Zhou, P.; Ma, B.; Zhao, J.; Song, J. Efficient photocatalytic H2 evolution catalyzed by an unprecedented robust molecular semiconductor {Fe11} nanocluster without cocata-lysts at neutral conditions. *Nano Energy* **2015**, *16*, 247−255.

(40) Huang, P.; Qin, C.; Su, Z.-M.; Xing, Y.; Wang, X.-L.; Shao, K.-Z.; Lan, Y.-Q.; Wang, E.-B. Self-assembly and photocatalytic properties of polyoxoniobates:{Nb$_{24}$O$_{72}$},{Nb$_{32}$O$_{96}$}, and {K$_{12}$Nb$_{96}$O$_{288}$} clusters. *J. Am. Chem. Soc.* **2012**, *134* (34), 14004−14010.

(41) Li, S.; Liu, S.; Liu, S.; Liu, Y.; Tang, Q.; Shi, Z.; Ouyang, S.; Ye, J. {Ta$_{12}$}/{Ta$_{16}$} cluster-containing polytantalotungstates with remark-able photocatalytic H$_2$ evolution activity. *J. Am. Chem. Soc.* **2012**, *134* (48), 19716−19721.

(42) Chandler, C. J.; Deady, L. W.; Reiss, J. A. Synthesis of some 2,9-disubstituted-1,10-phenanthrolines. *J. Heterocycl. Chem.* **1981**, *18* (3), 599−601.

(43) Angeloff, A.; Daran, J. C.; Bernadou, J.; Meunier, B. The Ligand 1,10-Phenanthroline-2,9-dicarbaldehyde Dioxime can Act Both as a Tridentate and as a Tetradentate Ligand− Synthesis, Characterization and Crystal Structures of its Transition Metal Complexes. *Eur. J. Inorg. Chem.* **2000**, *2000* (9), 1985−1996.

(44) Derakhshanrad, S.; Mirzaei, M.; Najafi, A.; Ritchie, C.; Bauzá, A.; Frontera, A.; Mague, J. T. Surface-grafted lanthanoid complexes of the tungstosilicate polyanion [SiW$_{12}$O$_{40}$]$^{4−}$: a synthetic, structural and computational investigation. *Acta Crystallogr., Sect. C: Struct. Chem.* **2018**, *C74* (11), 1300−1309.